

Dynamics of gravity-induced gradients in soap film thicknesses

G. Ropars,^{a)} D. Chauvat, and A. Le Floch

Laboratoire d'Electronique Quantique-Physique des Lasers, Unité Mixte de Recherche du Centre National de la Recherche Scientifique 6627, Université de Rennes 1, Campus de Beaulieu, F-35042 Rennes Cedex, France

M. N. O'Sullivan-Hale and R. W. Boyd

The Institute of Optics, University of Rochester, Rochester, New York 14627

(Received 23 November 2005; accepted 8 May 2006; published online 7 June 2006)

We demonstrate a direct measurement of thickness gradients in vertical soap films with a resonant differential interferometer, i.e., the Jamin-Fabry-Perot interferometer. Two regimes are investigated: thick colored films with gravity- and capillarity-induced gradients, and silvery-gray to common black films which are quasi-independent of gravity. In the colored zone, our differential method is an ideal tool with which to isolate the large thickness instabilities of the film reaching 17 nm/mm that characterize the end of its drainage. Using the so-called F^2 law of such an interferometer, thermal-induced thickness variations as small as 1 nm are isolated in the gradient-free common black film. © 2006 American Institute of Physics. [DOI: 10.1063/1.2209201]

Thin films, first studied by Newton,¹ and then extensively investigated, in particular, by Gibbs² and Mysels *et al.*,³ have received much attention in the last decade both for fundamental interest in turbulent effects⁴⁻⁸ and for applications including cell membranes in biology or foams in industry.⁹ Different optical methods have been used for their study such as laser-based two-wave interferometry in transmission,¹⁰⁻¹² reflection,¹³ or even IR absorption.¹⁴ Unfortunately, although these techniques allow good temporal resolutions, all these methods probe the film point by point but do not provide any information about the spatial gradients which govern the film dynamics. Here we show that the recently introduced dual multiwave interferometer, i.e., the so-called Jamin-Fabry-Perot (JFP) interferometer,¹⁵ is an ideal tool for such investigations.

It is well known that when a soap film drains from its support under gravity and capillary action, typically two zones can be observed when illuminated by white light: a zone with colored parallel fringes followed by a zone which does not reflect light, and a so-called black zone. This black film can be a relatively thick common black film or a microscopically thin Newton black film. As reported in many studies, the transition between these colored and black zones is accompanied by instabilities that are difficult to isolate. Here we make such a film using a simple and widely used solution: a commercial soap with glycerine and water. From a bath of the solution we draw a film of 10 cm height and 6 cm width with a metallic frame. Then, the motion of the frame is stopped and we obtain a mobile surface film during its drainage, as depicted in Fig. 1. The boundary between the colored zone and the black one, schematized by the thick straight line, moves continuously downward in time. While the film drains, distinct horizontal fringes develop indicating a thin flat film near the upper frame border and a thicker curved film merging with the bulk solution.

One of the main parameters of those films is of course their thickness. Previous optical studies performed to measure it, either in reflection, transmission, or absorption

modes, have used progressive waves in single or at most double pass and are thus limited in sensitivities. Here we propose an experimental setup (see Fig. 1) that has the following advantages. First, it uses multiple wave interferences of a Fabry-Perot cavity, which improves the sensitivity of the measurement by roughly the finesse F of the cavity. Second, it is a dual interferometer able to *simultaneously* probe two points of the film, and thus it gives direct access to the thickness *gradient* between the two points. By simply rotating the two crystals inside the cavity, the ordinary and extraordinary probe points can be separated vertically or horizontally.

In the actual experimental setup, the interferometer is injected by a frequency-monomode Innolight neodymium-doped yttrium aluminum garnet (Nd:YAG) laser operating at $\lambda_0=1.064 \mu\text{m}$. The JFP interferometer is designed with two 20 mm long antireflection-coated YVO_4 crystals giving a 3 mm separation between the ordinary (o) and extraordinary (e) beams, and two 99% reflectivity mirrors with a radius of

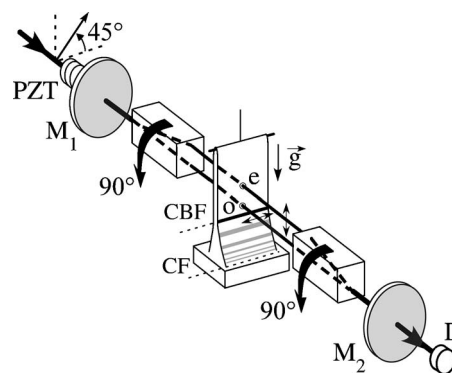


FIG. 1. Experimental setup. Linearly polarized and longitudinally monomode Nd:YAG laser light operating at $\lambda_0=1.064 \mu\text{m}$ is injected into the interferometer consisting of two 99% reflectivity mirrors (M_1 and M_2) with a radius of curvature $R_c=200 \text{ mm}$. A piezoelectric transducer (PZT) varies the length of the cavity. The two birefringent YVO_4 crystals give a 3 mm separation between the ordinary (o) and extraordinary (e) beams. The laser polarization is set 45° to the axes of these crystals. By rotating the two crystals by 90° , the probe points can be separated horizontally. The boundary between the colored film (CF) and the common black film (CBF) is schematized by the thick straight line. D is a detector.

^{a)}Electronic mail: guy.ropars@univ-rennes1.fr

curvature $R_c=200$ mm. Note that the distance between the two beams may be reduced to reach the beam waist of the interferometer which is here equal to 0.2 mm. Then the ordinary and extraordinary arms of the whole interferometer can exhibit transmission resonances. Namely, for each ordinary or extraordinary arm, the output intensity is written as $I_i(L, \ell_i^{\text{eff}}) = I^{\text{max}} / \{1 + m \sin^2[\phi_i^{\text{sp}}(L, \ell_i^{\text{eff}})]\}$, where $m = 2F/\pi$, where F is the finesse of the cavity, $\phi_i^{\text{sp}}(L)$ is the phase shift for one pass in the cavity, and $i=o, e$. This phase shift depends linearly on the length L of the cavity and on the optical or effective thickness ℓ_i^{eff} of the soap film in arm i . This effective thickness ℓ_i^{eff} is equal to $(n-1)\ell_i$, where n is the index of the film material and ℓ_i is the geometrical thickness of the film.¹⁶ The values of these two effective thicknesses are obtained from our measurements as shown below. We choose a confocal cavity configuration and measure a finesse of about 30. The separation $h=3$ mm between the two arms is well suited to probe the film gradients, as confirmed by visual observation of fringe dimensions. This gradient is given by

$$\frac{d\ell^{\text{eff}}}{dz} \approx \frac{\ell_o^{\text{eff}} - \ell_e^{\text{eff}}}{h} \quad (1)$$

and can be expressed in nm/mm. A charge-coupled device (CCD) camera captures in real time the evolution of the film during its drainage and is correlated to the acquisition of the ordinary and extraordinary path signals of the interferometer, which allows one to deduce the effective thickness of the film for the ordinary and extraordinary paths as shown below. The acquisition setup has a time response of 0.1 s, which is well adapted to the temporal evolution of the film. Note that the ultimate limitation of the temporal resolution is fixed by the photon lifetime in the cavity which is estimated to be 10^{-6} s. Finally the whole interferometer can be prepared either in a nondegenerate or a degenerate state of the resonant frequencies of the two ordinary and extraordinary modes by slightly tilting one of the two crystals.

Let us first consider the nondegenerate case. In Fig. 2(a), the two beams are vertically separated. As the length of the Fabry-Perot cavity is scanned with a piezoelectric transducer, the output signal of the interferometer shows two different resonant frequencies (see insets), each one corresponding to a maximum transmission peak of the ordinary or extraordinary beam path. These two peaks individually measure the effective thickness of the film. Indeed, as the film drains, these peaks shift continuously at different rates as shown by the arrows of the inset in Fig. 2(a). Note that although the height of the peaks can also vary due to the residual reflectivity of the film walls, it is only their frequency positions which are relevant here. It allows us to follow the thickness variations as a function of time as shown in the two curves in Fig. 2(a). When we pass from the colored zone to the silver-black one as discussed by Mysels *et al.*,³ the thickness varies rapidly from 600 to about 50 nm, then stabilizes around this value. Finally a collapse is forced at $t=20$ s in order to obtain an absolute zero for the thickness measurement. Note that since the index characterizing the film is known, we can also deduce the geometrical or absolute values of the film thickness. Although the two thickness variations appear similar in Fig. 2(a), when we directly measure the relative position of the two resonance peaks, we obtain a direct measurement of the thickness gradient during the whole evolution of

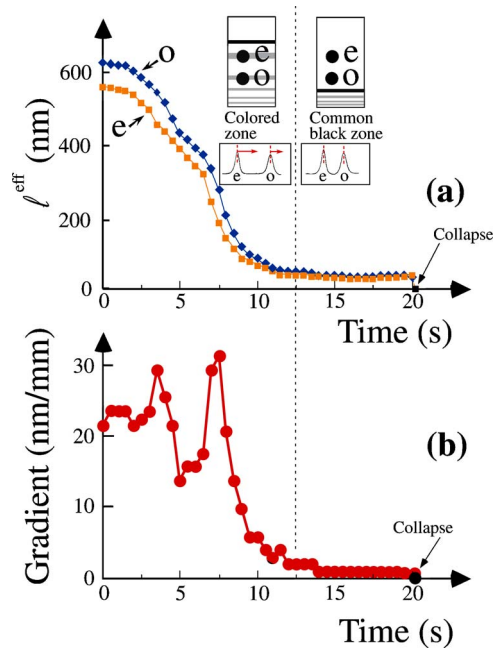


FIG. 2. (Color online) Effective thicknesses and gradients for vertically separated beams. (a) Effective thicknesses of the soap film for the ordinary and extraordinary beams vs time during drainage. The insets show typical extraordinary and ordinary Airy functions of the interferometer vs the cavity length at two different times. (b) Corresponding thickness gradients vs time showing large variations in the colored zone of the film and a nearly vanishing gradient in the black zone.

the film. Three features appear clearly: (i) in the colored zone, a large average value of the thickness gradient of 20 nm/mm for a 3 mm separation of the probe points, (ii) giant fluctuations reaching a peak-to-peak value of 17 nm/mm, and finally (iii) a quasinull gradient in the black zone.

In order to check that only vertical displacements exhibit such gradients, we now rotate both YVO_4 crystals by 90° around the laser beam propagation axis so that the two probe beams are now horizontally separated (cf. Fig. 1). As shown in Fig. 3, the two measured thickness curves are quasi-identical and now, when the differential measurement is performed, the gradient is negligible from the colored zone through the transition to the common black zone. In this black zone, one can note that the position of each peak maximum is very stable. The small fluctuations (about 0.5 nm/mm) observed in the gradient curve in the black zone could be attributed to small turbulence effects in the film.

While we have already gained sensitivity thanks to the finesse F of the Fabry-Perot, our experimental setup can show a still higher sensitivity. This can be achieved simply by measuring the output of the dual interferometer through use of an additional polarization analyzer in front of the detector in the frequency degenerate regime. In this case, the two transmission peaks are made to overlap by a slight tilt of one YVO_4 crystal. Then the analyzer is set either parallel or perpendicular to the input polarization. We observe a large transmission peak due to constructive interference between the ordinary and extraordinary states of the interferometer (see inset in Fig. 4) when the analyzer is set parallel to the input polarization, and we obtain destructive interference leading to a null signal (inset in Fig. 4) when the polarizer is perpendicular. This latter case allows a dark-field detection.

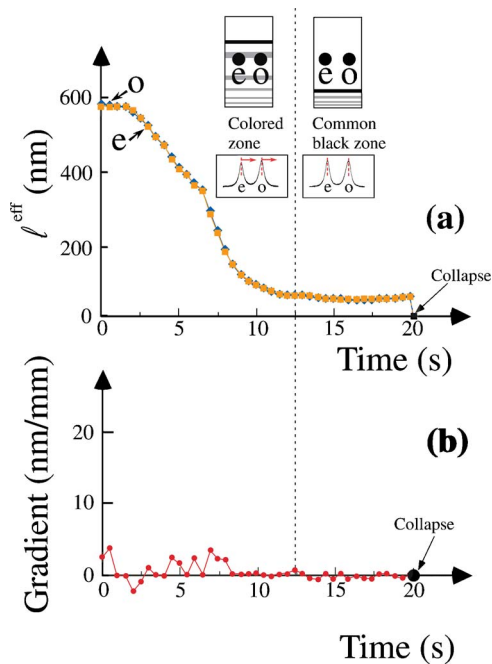


FIG. 3. (Color online) Effective thicknesses and gradients for horizontally separated beams. (a) Effective thicknesses of the soap film for the ordinary and extraordinary beams vs time. During the drainage of the soap film, the distance between the two Airy functions is constant, as shown in the insets. (b) Corresponding thickness gradients vs time, showing a nearly constant value.

If now a small phase shift $\Delta\Phi$ is added to one arm of the JFP, then a signal proportional to $(F\Delta\Phi)^2$ is detected. By slightly rotating the analyzer, the signal can also be made linear in $\Delta\Phi$ and the signal-to-noise ratio optimized. This enhanced sensitivity now allows us to measure very small effective

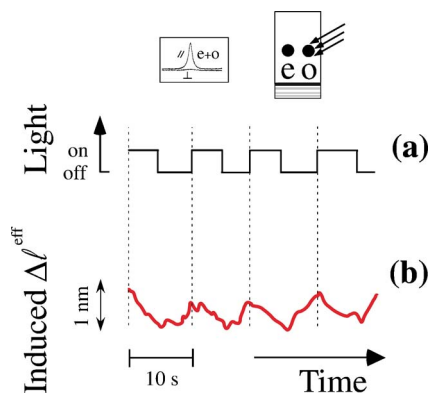


FIG. 4. (Color online) Measurement of small thickness variations of the film by local heating. (a) Thermal light intensity focused on the ordinary path on the film vs time. The inset shows the two superimposed Airy functions obtained by a slight tilt of one crystal and with a polarization analyzer set parallel (\parallel) and perpendicular (\perp) to the input polarization showing constructive and destructive interferences, respectively. (b) Corresponding induced thickness variations vs time.

thickness variations of the film, such as the known thinning induced by locally heating the film with thermal light.⁹ To this aim, we focus a thermal light source on the film at a point probed by only one of the two incident beams. We record the maximum intensity of the transmission peak through the analyzer. To increase the signal-to-noise ratio, the thermal light is chopped. As shown in Fig. 4, when the thermal light source irradiates the film, the thickness is smaller than when the source is off. According to the transmitted intensity variation, we deduce a corresponding thickness variation of 1 nm.

We have demonstrated that the JFP interferometer is well suited for the study of soap films, giving access to the thickness of the film and its gradient between two points. It allows one to study the role of instabilities which appear at the end of drainage of the film and to analyze both colored and black regimes of the film life. If the finesse of the interferometer is further increased, for instance, to a value of about $F=300$, and a synchronous detection is used to detect the maximum of the transmission peak, small thickness variations reaching the atomic scale, i.e., 0.1 nm, could be measured. Therefore the JFP interferometer should be a powerful tool for the important study of microscopically thin Newton black films. Moreover, a wide variety of other almost transparent objects with natural thickness gradients could be investigated with the JFP, in particular, in the realm of soft matter and biology.

The authors would like to thank J. J. Benattar for his constructive discussions. This work was supported jointly by the U.S. National Science Foundation under Grant No. INT-0003636, by CNRS Grant No. 10675, and by the Contrat de Plan Etat-Région (GIS FOTON).

- ¹I. Newton, *Optiks Book II* (Smith and Watford, London, 1704), pt. 1.
- ²J. W. Gibbs, *Collected Works* (Longmans, Green, New York, 1928), Vol. 1, p. 300.
- ³K. J. Mysels, K. Shinoda, and S. Frankel, *Soap Films: Studies of their Thinning* (Pergamon, New York, 1959).
- ⁴P. G. De Gennes, *Langmuir* **17**, 2416 (2001).
- ⁵E. Ruckenstein and M. Manciu, *Langmuir* **18**, 2727 (2002).
- ⁶V. Casteletto, I. Cantat, D. Sarker, R. Bausch, D. Bonn, and J. Meunier, *Phys. Rev. Lett.* **90**, 048302 (2003).
- ⁷F. Bresme and J. Faraudo, *Langmuir* **20**, 5127 (2004).
- ⁸Y. Amourachene and H. Kellay, *Phys. Rev. Lett.* **93**, 214504 (2004).
- ⁹J. J. Benattar, Q. Shen, S. Bratskaya, V. Petkova, M. P. Krafft, and B. Pucci, *Langmuir* **20**, 1047 (2004).
- ¹⁰V. Greco and G. Molesini, *Meas. Sci. Technol.* **7**, 96 (1996).
- ¹¹O. Greffier, Y. Amarouchene, and H. Kellay, *Phys. Rev. Lett.* **88**, 194101 (2002).
- ¹²C. Berger, V. Bergeron, B. Desbat, D. Blaudez, H. Kellay, and J.-M. Turlat, *Langmuir* **19**, 8615 (2003).
- ¹³S. Berg, E. A. Adelizzi, and S. M. Troian, *Langmuir* **21**, 3867 (2005).
- ¹⁴X. L. Wu, R. Levine, M. Rutgers, H. Kellay, and W. I. Goldberg, *Rev. Sci. Instrum.* **72**, 2467 (2001).
- ¹⁵D. Chauvat, C. Bonnet, A. Durand, M. Vallet, and A. Le Floch, *Opt. Lett.* **28**, 126 (2003).
- ¹⁶Actually, due to small constructive interferences in the film, the effective thickness is equal to $e_i^{\text{eff}} = K(n-1)e_i$, with $K = (3n^2 + 1)/(n+1)^2 \approx 1.16$ for a film of water.